Available online at www.sciencedirect.com
SCIENCE DIRECT®
Journal of Photochemistry and Photobiology A: Chemistry 179 (2006) 176–183
Journal of Photochemistry and Photobiology A:Chemistry
www.elsevier.com/locate/jphotochem

Photochemistry of the Fe(III)–EDTA complexes A mechanistic study

Przemysław Kocot, Andrzej Karocki, Zofia Stasicka *

Faculty of Chemistry, Jagiellonian University, Ingardena 3, 30-060 Kraków, Poland

Received 14 March 2005; received in revised form 15 July 2005; accepted 12 August 2005
Available online 19 September 2005

Abstract

The Fe(III) photoreduction in the EDTA complexes studied by pulse photolysis and continuous irradiation revealed that LMCT excitation is followed by reaction of the primary photoproduct with the parent complex, generating intermediate species formulated as $[(H_2O)(EDTA^{\bullet+})Fe^{II}(\mu\text{-}OH_x)Fe^{III}EDTA]^{x-4}$. The presence of molecular oxygen is of crucial relevance for the intermediate life time and pathway of decay. In deoxygenated media, the intermediate is relatively long-lived ($k_{obs} \sim 1 \times 10^{-3}\ s^{-1}$) and its degradation proceeds by the back electron transfer regenerating the parent complex and by the second inner-sphere electron transfer producing Fe(II) species and EDTA oxidation products. In this case the product ratio of the Fe(II) to $(EDTA)_{ox}$ should be 2:1, consistent with the previous reports.

In the presence of molecular oxygen, the intermediate dimer decomposes much faster ($k_{obs} \sim 1.4 \times 10^{2}\ s^{-1}$), presumably via outer-sphere two-electron oxidation of the dangling $CH_2COO^{\bullet}$ group and the Fe(II) centre, yielding $[Fe^{III}EDTA]^{-}$, $[Fe^{III}ED3A]$ and EDTA oxidation products. Formation of the $[Fe^{III}ED3A]$ complex was recorded only when Fe(III)–EDTA was irradiated in the presence of O_2. Under prolonged irradiation, it undergoes photoredox reaction resulting in oxidation of successive EDTA fragments and Fe_{aq}^{3+} production. Thus, in aerated media EDTA is oxidized by O_2 in the photocatalytic process, in which Fe(III) species plays a role of photocatalyst.

Quantum yields of the Fe(III)–EDTA decay depend on the irradiation wavelengths and solution pH; in deoxygenated media, the post-irradiation substrate regeneration makes the measured quantum yields apparently dependent on measurement time ($\phi_0 \approx 4\text{–}5\phi_\infty$).

Keywords: Fe(III)EDTA; EDTA photodegradation; LMCT photoreduction; Photoinduced electron transfer; Post-irradiation effect

1. Introduction

Iron compounds play an important role in environmental and biochemical systems, where interconversion between their main oxidation states proceeds readily. Fe(II) is oxidized by molecular oxygen, whereas Fe(III) is photoreduced by sunlight at the expense of its ligands or other sacrificial donors present in the medium. These reactions are integral parts of the Fe(III)/Fe(II) photocatalytic cycle, in which organic pollutants undergo degradation [1].

For some recalcitrant organic compounds, e.g. ethylenediaminetetraacetate (EDTA) and its derivatives, the photochemical oxidation is often the only way of its removal under environmental conditions. Neither conventional chemical nor biological wastewater treatment removes effectively EDTA, which is released to natural waters in relatively large amounts [2]. The advanced oxidation processes (AOP) have been developed, such as photocatalytic EDTA degradation with TiO_2 [3] or decomposition under UV light in the presence of H_2O_2 (photo-Fenton) [4–10]. It was reported earlier that in the case of the Fe(III)–EDTA complex the direct photolysis itself is also effective enough to abate the EDTA pollution; a minor role was assigned to $[Mn^{II}EDTA]^{2-}$ and $[Co^{III}EDTA]^{-}$ [12]. Recently, also the $[CrEDTA]^{-}$ complex was reported to show a similar behaviour, although with a relatively low yield [13].

The molecular structure of the Fe–EDTA complexes is complicated due to their two different coordination modes suggested for solid phases and solutions. In the crystalline Fe(III) salts EDTA is usually hexadentate and water molecule is coordinated as seventh ligand, forming approximate pentagonal-bipyramidal structure [14–21]. In the protonated form, $[FeH(EDTA)(H_2O)]$, a pentadentate six-coordinate geometry with EDTA containing

* Corresponding author. Tel.: +48 12 6335392.
E-mail address: stasicka@chemia.uj.edu.pl (Z. Stasicka).

1010-6030/$ – see front matter © 2005 Elsevier B.V. All rights reserved.
doi:10.1016/j.jphotochem.2005.08.016

one uncoordinated, protonated carboxylic group was also suggested [22].

Further studies [23–29] have demonstrated that the structures are retained in solutions exhibiting characteristic acid–base equilibria. In the pH range typical for the environmental systems (4–9) the equilibrium involves two forms:

$$[FeEDTA(H_2O)]^- + OH^- \rightleftarrows [FeEDTA(OH)]^{2-} + H_2O \quad (1)$$

with pK_1 value within the 7.4–7.8 at 25 °C [11,14,15,18,19,30,33]. Besides the monomeric Fe(III)–EDTA complexes, also an oxo-bridged dimer:

$$2[FeEDTA(OH)]^{2-} \rightleftarrows [EDTAFe(\mu\text{-}O)FeEDTA]^{4-} + H_2O \quad (2)$$

with a pentadentate six-coordinate geometry, was identified in the solid phase and in moderately concentrated alkaline solutions ($c \geq 1$ mM) [18,19,26,31–35].

Direct photochemistry of the Fe(III)–EDTA system was studied repeatedly. The Fe(II) species, CO_2 and HCHO were identified as the final products of the Fe(III)–EDTA photoreduction in solid salts or in deoxygenated solutions [30,35–37]. The quantum yield ratio, $\phi(Fe^{2+}):\phi(CO_2):\phi(HCHO) \approx 2:1:1$ suggested a rapid thermal reduction of the substrate by the primary photolysis product according to overall reaction [30]:

$$2[Fe^{III}EDTA]^- \xrightarrow{h\nu} [Fe^{II}EDTA]^{2-} + Fe^{II}\cdot aq + ED3A^{3-} + CO_2 + HCHO \quad (3)$$

Opposite to EDTA, its photodegradation products were reported to be biodegradable [12]. A more detailed product analysis has shown that prolonged irradiation of aerated solutions yields EDTA photodegradation products, such as ethylenediaminetriacetic acid (ED3A), ethylenediaminediacetic acids (EDDA-*N*,*N*′ and EDDA-*N*,*N*), ethylenediaminemonoacetic acid (EDMA), imidoacetic acid (IMDA) and glycine. Similar decomposition products were identified for the Fe(III)–DTPA complex (DTPA: diethylenetriaminepentaacetic acid) [38].

The rate of the Fe(III)–EDTA photoreduction was analysed as a function of radiation wavelength, pH, presence of oxygen and temperature. The quantum yields appeared to be susceptible to various parameters, such as irradiation wavelength, light intensity and substrate concentration [11,30,35]. The molecular oxygen was claimed to increase the ϕ value but the effect could not be interpreted unambiguously [11].

The effect of pH was studied a few times and in most papers the enhanced photolysis efficiency at low pH was reported [7,12], whereas more recent results showed that ϕ values measured at 405, 366 and 313 nm were independent of pH over the range $4 \leq pH \leq 9$ [11].

More extensive investigations of the Fe(III)–EDTA photochemistry were performed by Natarajan and Endicott [30] and Kari et al. [11], unfortunately their experimental conditions were completely different: the former study was carried out in relatively concentrated deoxygenated solutions, whereas the latter—in extremely diluted solutions in the presence of an O_2 excess. The results cannot be therefore comparable.

Thus, although a number of kinetic information and corresponding considerations are available, some mechanistic details still remain unclear and call for further clarification. This knowledge is important mainly because of the environmental relevance of the Fe–EDTA photochemistry, where such parameters as pH and concentration of substrate and/or O_2 can vary within wide limits.

In this study, a more detailed investigations of O_2 and pH influence on the Fe–EDTA photochemistry was performed. Our investigation possibly does not fill all gaps in this area but supplies some more data, which can be satisfactorily interpreted.

2. Experimental

2.1. Chemicals

All reagents of highest available purity were used as purchased. Solutions of all reagents were freshly prepared using triply distilled water or demineralised by Millipore Milli Q Plus filter. Aqueous solutions of $1–15 \times 10^{-5}$ M Na[FeEDTA]·2H_2O were used in Britton–Robinson buffer containing 0.04 M H_3PO_4, 0.04 M H_3BO_3, 0.04 M CH_3COOH and NaOH, adjusted to pH 4 and 9. Oxygen-free and oxygenated solutions were made by saturation with argon or molecular oxygen, respectively, over at least 30 min. All measurements were performed at 293 and 303 ± 0.1 K.

2.2. Instrumentation and procedures

UV–vis spectra were recorded in thermostated 1 cm quartz cells using a Shimadzu UVPC 2100 or a Hewlett-Packard HP 8453 spectrophotometer. PH values were measured using a CX-741 Elmetron pH-meter with a glass electrode.

Irradiations were carried out using a low-pressure mercury lamp as source of 254 nm radiation and a high-pressure mercury HBO-200 lamp equipped with interference 365 or 313 nm filter. Differential quantum yields $\phi = \frac{d[c]/dt}{n}$ (where $d[c]/dt$ is the rate of the Fe(III)–EDTA concentration change and n is amount of einsteins absorbed per unit time) were determined using a trisoxalatoferrate(III) actinometer [40].

Pulse photolysis in the millisecond time scale was performed using a LKS 60 Spectrometer (Applied Photophysics) equipped with Nd-YAG laser pump source Surelite I-10 (Continuum), operating in fourth harmonic (266 nm, max 75 mJ pulses, 6 ns FWHM). Data were recorded on a digital storage oscilloscope HP 54522A with 0.5 ns time resolution and transferred to a computer for subsequent handling.

Factor analysis of the irradiated solution spectra was performed using Target 96M software (MATLAB version) [39]. This method is based on algorithm of decomposition of the experimental spectroscopic information recorded as matrix into the concentration and molar absorbance matrices, which correspond to the Beer–Lambert's law as follow:

$$\mathbf{A}(p \times q) = \mathbf{C}(p \times n) \times \mathbf{E}(n \times q),$$

where **A** is the experimental matrix, **C** the concentration matrix and **E** is the matrix of molar absorption coefficients. Their sizes are indicated in the parentheses where n, p and q are a numbers of absorbing species, samples and wavelengths, respectively. Input matrix A was built from 12 experimental spectra obtained in individual experiments.

3. Results and discussion

The study is focused on the photochemical behaviour of two main forms of the Fe(III)–EDTA species, which prevail in the nature, i.e. aqua $[Fe^{III}EDTA(H_2O)]^-$ (investigated at pH 4) and hydroxo $[Fe^{III}EDTA(OH)]^{2-}$ (at pH 9). The substrate concentrations ($1–15 \times 10^{-5}$ M) were kept low enough to avoid the oxo-bridged dimer formation in the thermal reaction (Eq. (2)), but high enough to enable noticeable consumption of the second substrate molecule upon excitation (cf. Eq. (3)).

The electronic spectra of the complexes are characterized by an intense LMCT bands at $\lambda_{max} = 258$ nm ($\varepsilon_{max} = 8530\ M^{-1}\ cm^{-1}$) and $\lambda_{max} = 248$ nm ($\varepsilon_{max} = 8170\ M^{-1}\ cm^{-1}$) for $[Fe^{III}EDTA(H_2O)]^-$ and $[Fe^{III}EDTA(OH)]^{2-}$ forms, respectively, which are in agreement with the values reported earlier [8,11,19,28,41]. Irradiation within the absorption bands leads to decrease in absorption characteristic of the parent Fe(III) complex, consistent with its anticipated reduction to Fe(II) [30,35,37].

The reduction initiated by the photoinduced electron transfer (PET):

$$[Fe^{III}EDTA(H_2O)]^- \xrightarrow{h\nu(LMCT)} [Fe^{II}EDTA^{\bullet}(H_2O)]^- \quad (4a)$$

$$[Fe^{III}EDTA(OH)]^{2-} \xrightarrow{h\nu(LMCT)} [Fe^{II}EDTA^{\bullet}(OH)]^{2-} \quad (4b)$$

is followed by the back electron transfer:

$$[Fe^{II}EDTA^{\bullet}(H_2O)]^- \rightarrow [Fe^{III}EDTA(H_2O)]^- \quad (5a)$$

$$[Fe^{II}EDTA^{\bullet}(OH)]^{2-} \rightarrow [Fe^{III}EDTA(OH)]^{2-} \quad (5b)$$

and by reactive decay of the transient radical species, which was recorded within milliseconds upon excitation by a 266-nm laser pulse. The results show that the most important factor determining the post-irradiation pathway is the presence of molecular oxygen; pH and substrate concentration are of minor significance.

In the absence of oxygen, a post-irradiation consumption of the parent complex is the first effect detected within milliseconds. The effect is illustrated in Fig. 1a showing the absorption changes recorded in deoxygenated solutions at pH 4. The reaction rate depends on the Fe(III)–EDTA concentration (Fig. 1b), consistent with the rapid thermal reduction of the substrate by the primary photolysis product (Eq. (3)) suggested earlier [30].

At longer delay times (within minutes), a partial regeneration of the substrate is observed (Fig. 2), proceeding with a moderate rate, which initial value ($k_{obs} \approx 1 \times 10^{-3}\ s^{-1}$) is nearly independent of pH (within 4–9) and temperature (within 292–302 K). This behaviour leads to considerably different reaction yields when substrate concentrations are measured immediately after switching the light off and after some time (Fig. 3). In consequence, the quantum yield values (ϕ), measured in deoxygenated solutions depend apparently on the measurement time. This is shown in Table 1, where ϕ_0 (extrapolated to the time of switching the light off), is ~4–5 times higher than ϕ_∞ (measured after ~2 h, i.e. time long enough to cease almost all post-irradiation processes). The considerable difference between ϕ_0 and ϕ_∞ is presumably the source of discrepancy in the quantum yield values reported earlier [11,37].

The post-irradiation effects imply a conclusion that the transient radical species produced by PET (4a,b) reacts fast with the substrate generating a relatively stable intermediate, presumably a dimeric species, e.g.

$$[Fe^{II}EDTA^{\bullet+}(H_2O)]^- + [Fe^{III}EDTA(H_2O)]^- \rightarrow [(H_2O)(EDTA^{\bullet+})Fe^{II}(\mu\text{-}OH_x)Fe^{III}EDTA]^{x-4} \quad (6)$$

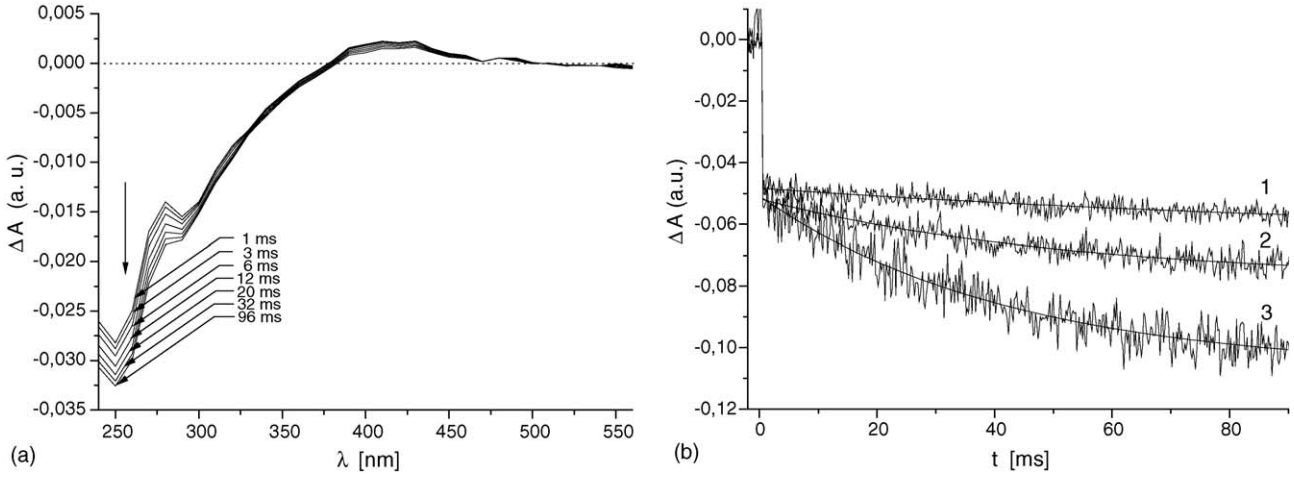

Fig. 1. (a) Time resolved spectra ($A_\tau - A_0$) recorded in deoxygenated 5×10^{-5} M solution of $[FeEDTA(H_2O)]^-$ at pH 4 upon excitation by a 266-nm laser pulse; the delay times are shown on the drawing; (b) kinetic traces at 250 nm recorded within milliseconds upon flashing of 5×10^{-5} (1), 1×10^{-4} (2) and 1.4×10^{-4} M (3) $[FeEDTA(H_2O)]^-$ solutions.

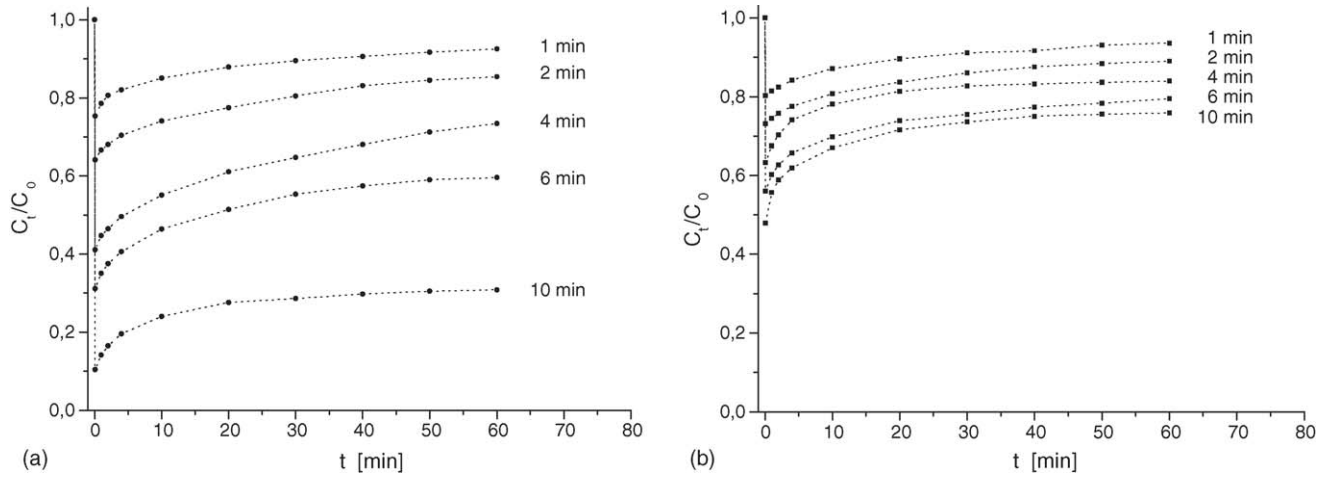

Fig. 2. Post-irradiation regeneration of the Fe(III)–EDTA parent complex after exposure of its deoxygenated 1×10^{-4} M solution to continuous 254 nm irradiation for 1, 2, 4, 6 and 10 min at pH 4 (a) and pH 9 (b) (measured at 302 K).

($x = 0$, 1 or 2). The back electron transfer reproduces the parent Fe(III) complex:

$$[(H_2O)(EDTA^{\bullet+})Fe^{II}(\mu\text{-}OH_x)Fe^{III}EDTA]^{x-4} \rightarrow 2[Fe^{III}EDTA(H_2O)]^- \quad (7)$$

whereas the second innersphere electron transfer from the $EDTA^{\bullet+}$ moiety to the Fe(III) centre results in formation of Fe(II) complexes and EDTA oxidation products:

$$[(H_2O)(EDTA^{\bullet+})Fe^{II}(\mu\text{-}OH_x)Fe^{III}EDTA]^{x-4} \rightarrow [Fe^{II}EDTA]^{2-} + Fe^{II}\cdot aq + ED3A^{3-} + CO_2 + HCHO \quad (8)$$

Oxygenation of the photolysed solution leads to rapid regeneration of the parent $Fe^{III}EDTA$ complex, which is in accordance with the EDTA effect on acceleration of the iron(II) autoxidation reported earlier [42–48]. However, because of the partial EDTA degradation, the regeneration of the parent complex is not complete.

The two-step mechanism of the Fe(III)–EDTA photoreduction (Eqs. (6) and (8)), and especially formation of the intermediate dimer, are justified by some additional arguments. (i) The photoinduced innersphere electron transfer from the EDTA ligand leads to formation of a vacant coordination site in the $[Fe^{II}(EDTA^{\bullet+})(H_2O)]^-$ or $[Fe^{II}(EDTA^{\bullet+})(OH)]^{2-}$ transient species, enabling coordination of the parent complex by means of its H_2O or OH^- ligand. (ii) As in the thermal dimerization [32–34,41], the photoinduced dimerization is favoured by the alkaline medium, i.e. the post-irradiation substrate consumption at pH 4 ceases at ~100 ms ($k_{obs} \sim 20\ s^{-1}$), whereas at pH 9 the process is finished within ~5 ms. Proton removal from the bridging O-atom is presumably the reason of such behaviour and more probable intermediate is the μ-OH or even μ-O-dimer. (iii) The intermediate formation is accompanied by an increase in absorption at $250 < \lambda < 500$ nm (with bands at

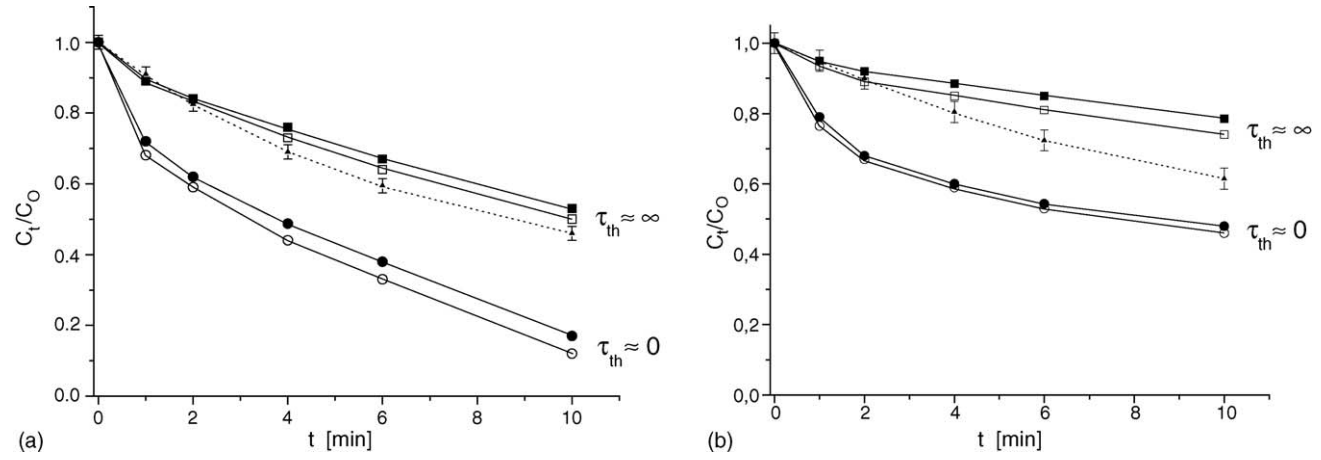

Fig. 3. Fe(III)–EDTA decay in function of irradiation time extrapolated to the time of switching the light off ($\tau_{th} \approx 0$, marked as circles) and recorded 100 min later, i.e. upon ceasing all post-irradiation thermal reactions ($\tau_{th} \approx \infty$, marked as squares); 1×10^{-4} M Fe(III)–EDTA was irradiated by a 254-nm line in deoxygenated solutions (full lines) and in oxygenated solutions (dotted lines, error bars show the scatter of results at different measurement times); empty symbols and dotted lines denote measurements at 292 K and filled symbols at 302 K; (a) applies to $[FeEDTA(H_2O)]^-$ at pH 4, whereas (b) to $[FeEDTA(OH)]^{2-}$ at pH 9.

Table 1
Effect of irradiation wavelength, pH and O_2 concentration on quantum yields of the Fe(III)–EDTA photoreduction (initial concentration 1×10^{-4} M, temperature 292 K)

Irradiation wavelength (nm)	pH	Oxygen concentration			
		Deoxygenated	Oxygenated	Ambient air	
254	4	$\phi_0 = 0.33 \pm 0.05$[a], $\phi_\infty = 0.09 \pm 0.01$[b] ~0.4[c]	0.11 ± 0.01	0.12 ± 0.01	
	9	$\phi_0 = 0.27 \pm 0.025$[a], $\phi_\infty = 0.05 \pm 0.006$[b]	0.04 ± 0.02	0.05 ± 0.01	
313	4	$\phi_0 = 0.09 \pm 0.010$[a] ~0.2[c]	0.05 ± 0.006	0.05 ± 0.007	0.082[e]
	9	$\phi_0 = 0.06 \pm 0.007$[a]	0.01 ± 0.002	0.01 ± 0.002	
350	9	0.065[d]	–	–	–
365	4	$\phi_0 = 0.06 \pm 0.005$[a] ~0.08[c]	0.02 ± 0.002	0.03 ± 0.002	0.034[e]
	9	$\phi_0 = 0.04 \pm 0.003$[a]	0.01 ± 0.001	0.01 ± 0.001	
405	4	~0.01[c]	–	0.018[e]	
	9	–	–		

[a] Extrapolated to the time of switching the light off.
[b] Measured 100 min upon switching the light off.
[c] Value for 2×10^{-3} M solution (estimated from Fig. 2 in Ref. [30]).
[d] Value for 0.3–4 $\times 10^{-2}$ M solution from Ref. [35].
[e] Value for $<10^{-6}$ M solution from Ref. [11].

~270 and 410 nm), which is relatively invariable within milliseconds (cf. Fig. 1a) and decays in minutes. The absorption can be assigned to the metal-to-metal charge transfer transition, resembling to some extent the $[EDTAFe(\mu\text{-}O)FeEDTA]^{4-}$ spectrum [18,19,34].

In the presence of molecular oxygen, the post-irradiation behaviour is radically different from that observed in the O_2 absence. This is illustrated in Fig. 4, where the absorption changes recorded within 20 ms upon laser pulse excitation of Fe(III)–EDTA in oxygenated solutions are compared with those observed for deoxygenated solutions at pH 4 (a) and 9 (b). In the presence of O_2, from the shortest observation time an increase in absorption is recorded which is independent of pH and is complete upon ~20 ms ($k_{obs} = 1.4 \times 10^2\ s^{-1}$).

The increase in absorption near 250 nm (shown in Fig. 4) could suggest fast regeneration of the initial Fe(III)EDTA complex [42–48]. Time resolved spectra of the oxidation product obtained in flash photolysis (Fig. 5) are, however, different from the initial spectrum: instead of maximum at 258 nm, the spectra are characterized by a discrete absorption band at ~300 nm and an increase in absorption at $\lambda > 270$ nm. Spectrum of the oxidation product generated in continuous photolysis was isolated from the photolyte spectra on two ways: by subtraction of the photolyte spectra recorded under exactly the same conditions except presence of oxygen ($A_{ox} - A_{deox}$, Fig. 6a), and by resolving the photolyte spectra to their components by means of the factor analysis [39] (Fig. 6b).

The results showed that in the presence of O_2 the same product is generated by flash and continuous photolysis, irrespective of pH and substrate concentration, which is characterised by an intense absorption with maximum about 280–300 nm and $\lambda > 250$ nm. The oxidation product was assigned to the $[Fe^{III}ED3A]$ complex, which production in aerated Fe(III)–EDTA systems was documented earlier

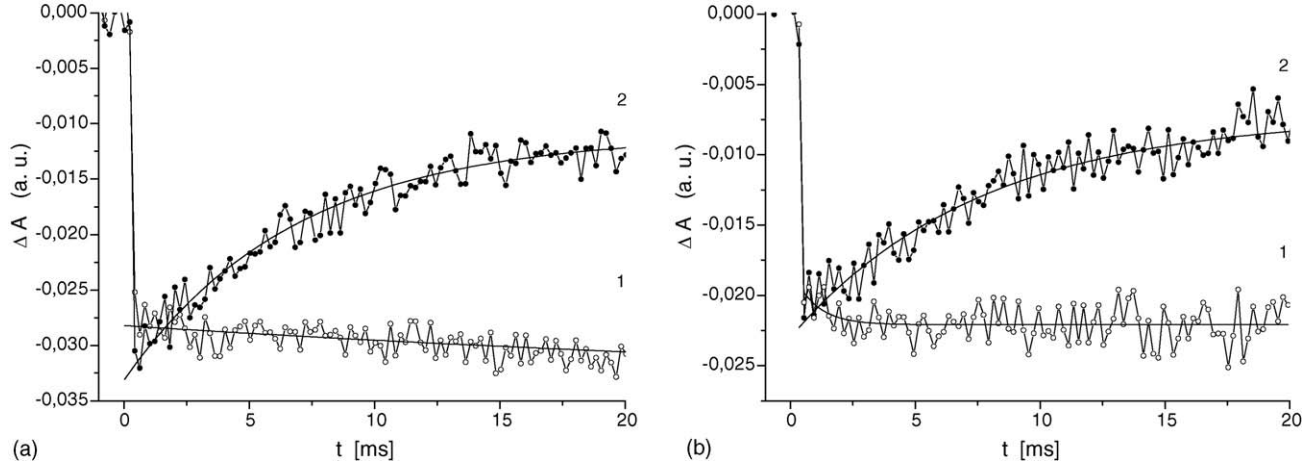

Fig. 4. Kinetic traces at 250 nm in deoxygenated (curve 1) and oxygenated (curve 2) 5×10^{-5} M solutions of $[FeEDTA(H_2O)]^-$ at pH 4 (a) and $[FeEDTA(OH)]^{2-}$ at pH 9 (b), recorded upon excitation by a 266-nm laser pulse.

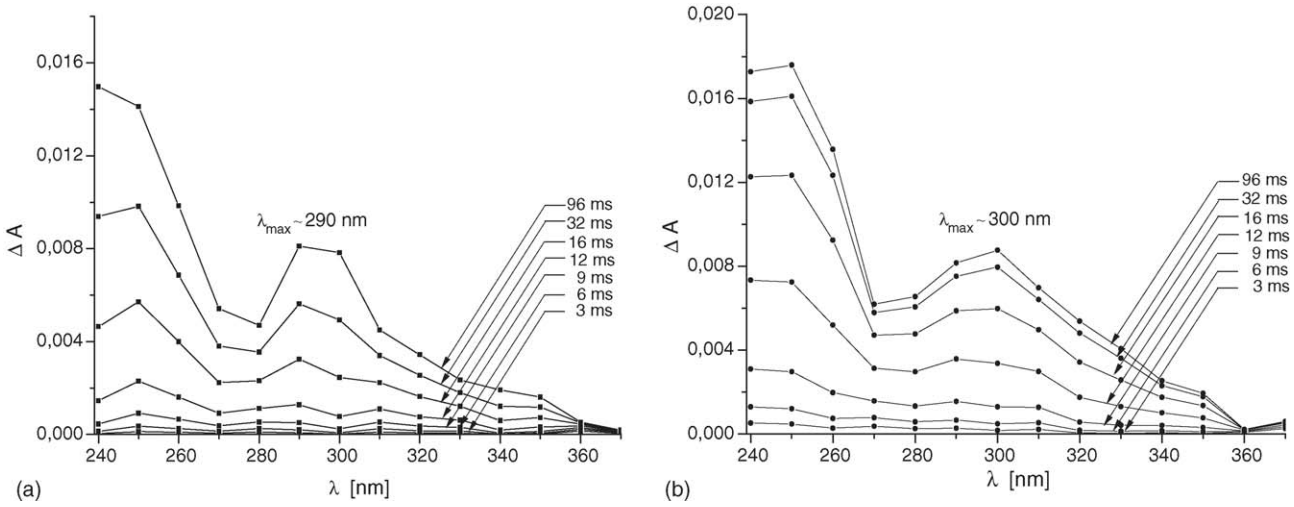

Fig. 5. Time resolved spectra ($A_\tau - A_i$, $i = 1$ ms, $\tau = 3$, 6, 9, 12, 16, 32, 96 ms) recorded in oxygenated 5×10^{-5} M solutions of $[FeEDTA(H_2O)]^-$ at pH 4 (a) and $[FeEDTA(OH)]^{2-}$ at pH 9 (b) upon excitation by a 266-nm laser pulse.

[7,9,12,30,37]. Its immediate formation can follow either a stepwise or concerted two-electron oxidation of the dangling $CH_2COO^\bullet$ radical moiety and the Fe(II) centre in the dimer intermediate. The results of this paper support the second possibility.

$$[(H_2O)(EDTA^{\bullet+})Fe^{II}(\mu\text{-}OH_x)Fe^{III}EDTA]^{x-4} \xrightarrow{O_2} [Fe^{III}ED3A] + [Fe^{III}EDTA]^- + CO_2 + HCHO + H_2O \quad (9)$$

The $[Fe^{III}ED3A]$ product is thermally stable, resistant to oxygenation but undergoes photodecomposition, leading upon prolonged irradiation to EDTA depletion and the aqua/hydroxo Fe(III) complex formation. Thus, the secondary thermal processes following the photoreduction regenerate fast the Fe(III) species, making the process of the EDTA degradation the photocatalytic one.

Quantum yields of the Fe(III) photoreduction (Table 1) depends on the irradiation wavelength: the yield is the higher the more energetic radiation within 254–365 nm, which is consistent with the tendency reported by previous authors [11,30,35]. The final product nature is insensitive to the irradiation wavelength, as the same final spectra are obtained upon the Fe(III)–EDTA exposure to 266 nm laser pulse or to continuous 254, 313, 365 nm irradiation or polychromatic simulated solar radiation ($\lambda_{irr} > 290$ nm).

Opposite to the previous report [11], the results of this paper demonstrate repeatable effect of the solution pH on the ϕ values, which in all cases are lower at higher pH values. The behaviour may has its origin in the back electron transfer within the dimer

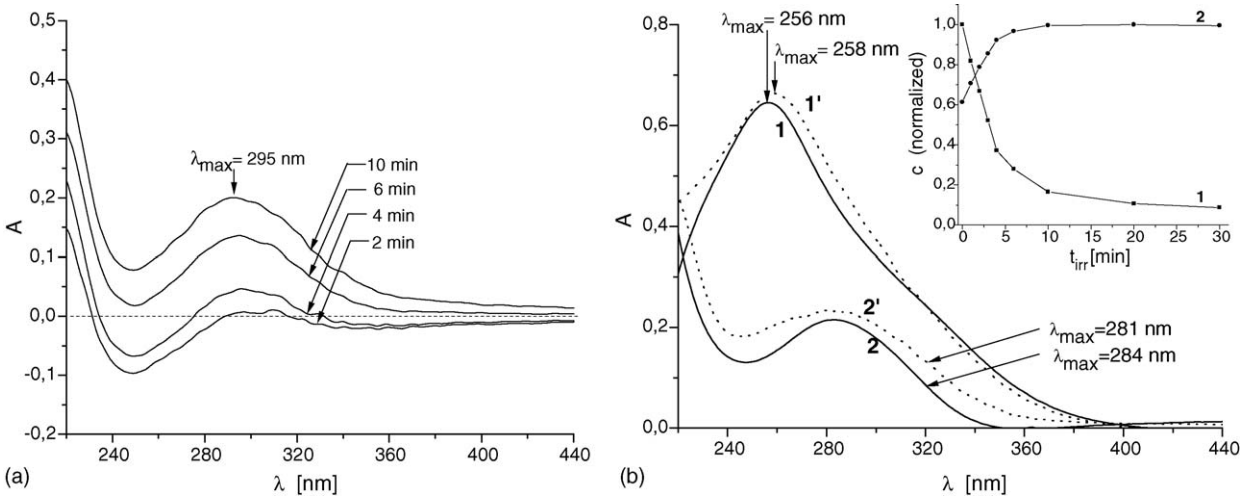

Fig. 6. (a) The differential spectra ($A_{ox} - A_{deox}$) of oxygenated and deoxygenated 1×10^{-4} M solutions of $[FeEDTA(H_2O)]^-$ at pH 4 upon continuous irradiation (254 nm) under exactly the same conditions (t_{irr} values are shown in the figure); and (b) results of resolving of the photolyte spectra obtained in the O_2 presence by means of factor analysis: spectra of the $[FeEDTA(H_2O)]^-$ substrate (curve 1) and oxidation product (curve 2) compared with those measured experimentally (dotted lines 1′ and 2′, respectively); insert to (b) shows concentration profiles of substrate (1) and product (2) during continuous irradiation.

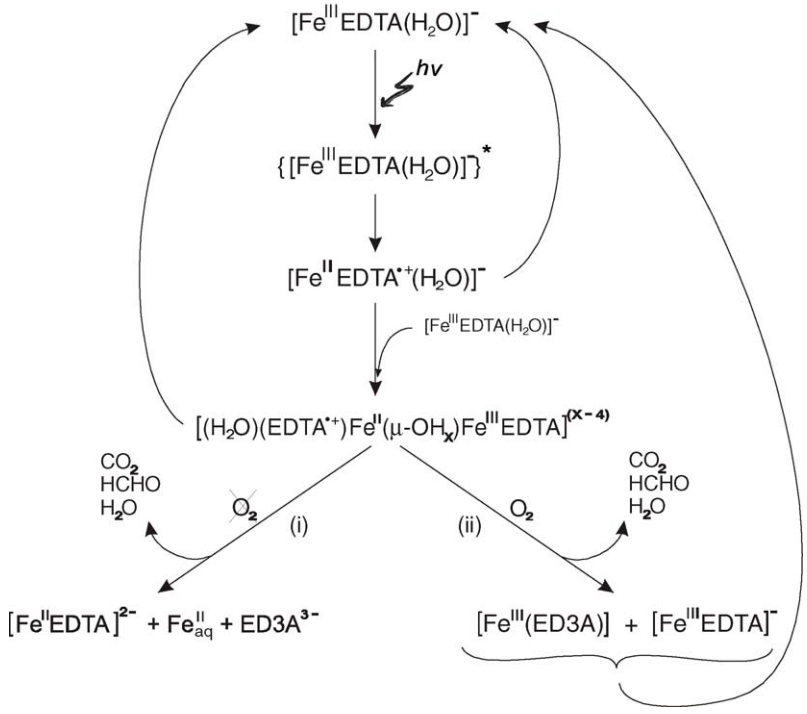

Scheme 1. Mechanistic pathways of the secondary thermal reactions proceeding in deoxygenated (i) and oxygenated (ii) solutions of $[FeEDTA(H_2O)]^-$ in a consequence of the LMCT excitation. (Mechanism of the reactions in the case of the $[Fe(OH)EDTA]^{2-}$ complex is supposed to be analogous.)

intermediate leading initially to formation of the [EDTAFe(μ-O)FeEDTA]$^{4-}$ dimer (Eq. (10)), which stability is increased at higher pH values.

$$[(H_2O)(EDTA^{\bullet+})Fe^{II}(\mu\text{-}O)Fe^{III}EDTA]^{4-} \rightarrow [EDTAFe(\mu\text{-}O)FeEDTA]^{4-} \quad (10)$$

Initial concentration of Fe(III)–EDTA should be of importance to the relative rates of the secondary thermal processes (Eqs. (6)–(10)), what seems to find some response in the literature results cited in Table 1.

The most crucial effect on the quantum yields is exerted, however, by molecular oxygen: in deoxygenated solutions the highest ϕ values are those extrapolated to the time of switching the light off, whereas after time long enough to cease the post-irradiation effect, the measured ϕ values drop to the values 4–5 times lower. Opposite, in the presence of molecular oxygen quantum yields measured at $t > 20$ ms, are constant within the measurement time and they are roughly similar to the ϕ_∞ values. These results justify the previous erroneous conclusion that oxygen has no real influence on the photoreduction process [11]. Nevertheless, from the mechanistic point of view the role of molecular oxygen is decisive both for the nature of the final products and for the EDTA photodegradation efficiency.

4. Conclusions

The study of fast post-irradiation processes of the Fe(III)–EDTA complexes in their excited LMCT states demonstrates that there are two main reaction pathways leading to EDTA oxidation (Scheme 1). The pathways originate from the same dimer intermediate, $[(H_2O)(EDTA^{\bullet+})Fe^{II}(\mu\text{-}OH_x)Fe^{III}EDTA]^{x-4}$, but differ the post-irradiation electron transfer from the $EDTA^{\bullet 3-}$ moiety: (i) in deoxygenated media the innersphere electron transfer to the Fe(III) centre yields Fe(II) species and EDTA oxidation products (Eq. (8)), whereas (ii) in aerated or oxygenated media the outersphere two-electron transfer to O_2 results in fast oxidation of the dangling $CH_2COO^{\bullet}$ group to CO_2 and HCHO, with the concerted regeneration of the Fe(III) in form of $[Fe^{III}ED3A]$ and the parent complex (Eq. (9)). The decay of the intermediate dimer in the intermolecular reaction with molecular oxygen is about 5 orders of magnitude faster than its intramolecular decomposition, what is consistent with the radical character of the reaction (Eq. (9)).

Moreover, the pathways differ substantially in the mechanism of the EDTA oxidation by Fe(III), which is stoichiometric only under deoxygenated conditions and consistent with the previous results [30,35] yields Fe(II) and CO_2, in the 2:1 ratio. In aerated or oxygenated media, however, EDTA is oxidized by O_2 in the photocatalytic process and its oxidation is accompanied by simultaneous Fe(III) regeneration. The results of this paper lead thus to conclusion that the EDTA oxidation in the presence of molecular oxygen is much more efficient.

Although the ϕ values decrease with the decrease of the radiation energy, they are high enough to enable the Fe(III)–EDTA photoreduction by the sunlight. As a consequence, the EDTA photodegradation can be the visible-light-driven process proceeding in the sunlit natural waters. Under aerated conditions, the Fe(III) species undergo very fast regeneration (Eq. (9)), what emphasizes the important role of the Fe(III)–EDTA system in the photocatalytic degradation of EDTA proceeding in the environment.

Acknowledgements

The financial support from the Polish State Committee for Scientific Research, PB Grant No. 4/T09A/181/24, is highly acknowledged. Authors thank also Dr. A. Turek for his help in numerical analysis of UV–vis spectra.

References

[1] P. Cieśla, P. Kocot, P. Mytych, Z. Stasicka, J. Mol. Catal. A 224 (2004) 17–33.
[2] S. Metsärinne, T. Tuhkanen, R. Aksela, Chemosphere 45 (2001) 949–955.
[3] P.A. Babay, C.A. Emilio, R.E. Ferreyra, E.A. Gautier, R.T. Gettar, M.I. Litter, Water Sci. Technol. 44 (2001) 179–185.
[4] A. Safarzadeh-Amiri, J.R. Bolton, S.R. Cater, Sol. Energy 56 (1996) 439–443.
[5] A. Safarzadeh-Amiri, J.R. Bolton, S.R. Cater, Water Res. 31 (1996) 787–798.
[6] J.J. Pignatello, Environ. Sci. Technol. 26 (1992) 944–951.
[7] S.H. Bossman, E. Oliveros, S. Göb, S. Siegwart, E.P. Dahlen, L. Payawan Jr., M. Straub, M. Wörner, A.M. Braun, J. Phys. Chem. A 102 (1998) 5542–5550.
[8] M. Sörensen, F.H. Frimmel, Z. Naturforsch. 50b (1995) 1845–1853.
[9] M. Sörensen, S. Zurell, F.H. Frimmel, Acta Hydrochim. Hydrobiol. 26 (1998) 109–115.
[10] G. Ghiselli, W.F. Jardim, M.I. Litter, H.D. Mansilla, J. Photochem. Photobiol. A: Chem. 167 (2004) 59–67.
[11] F.G. Kari, S. Hilger, S. Canonica, Environ. Sci. Technol. 29 (1995) 1008–1017.
[12] H.B. Lockhart Jr., R.V. Blakeley, Environ. Sci. Technol. 9 (1975) 1035–1038.
[13] P. Cieśla, A. Karocki, Z. Stasicka, J. Photochem. Photobiol. A 162 (2004) 537–544.
[14] J.L. Hoard, M. Lind, J.V. Silverton, J. Am. Chem. Soc. 83 (1961) 2770–2771.
[15] J.L. Hoard, C.H.L. Kennart, G.S. Smith, Inorg. Chem. 2 (1963) 1316–1317.
[16] M.D. Lind, M.J. Hamor, T.A. Hamor, J.L. Hoard, Inorg. Chem. 3 (1964) 34–43.
[17] L.H. Hall, J.L. Lambert, J. Am. Chem. Soc. 90 (1968) 2036–2041.
[18] M. Dellert-Ritter, R. van Eldik, J. Chem. Soc. Dalton Trans. (1992) 1037–1044.
[19] A. Brausen, R. van Eldik, Inorg. Chem. 43 (2004) 5351–5359.
[20] J.M. López-Alcalá, M.C. Puerta-Vizcaíno, F. González-Vílchez, Acta Cryst. C40 (1984) 939–941.
[21] X. Solans, M.F. Altaba, J. Garcia-Oricain, Acta Cryst. C40 (1984) 635–638.
[22] J.L. Lambert, Ch.E. Godsey, L.M. Setz, Inorg. Chem. 2 (1963) 127–129.
[23] J.F. Whidby, D.E. Leyden, Anal. Chim. Acta 51 (1970) 25–30.
[24] C. Manley, Z. Angew. Phys. 32 (1971) 187–193.
[25] J. Bloch, G. Navon, J. Inorg. Nucl. Chem. 42 (1980) 693–700.
[26] J. Oakes, E.G. Smith, J. Chem. Soc., Faraday Trans. 1 (1983) 543–552.
[27] K.C. Francis, D. Cummins, J. Oakes, J. Chem. Soc., Dalton Trans. (1985) 493–498.
[28] Ch. Bull, G.J. McClune, J.A. Fee, J. Am. Chem. Soc. 105 (1983) 5290–5300.
[29] K. Kanamori, H. Dohniwa, N. Ukita, I. Kanesaka, K. Kawai, Bull. Chem. Soc. Jpn. 175 (1990) 1447–1453.
[30] P. Natarajan, J.F. Endicott, J. Phys. Chem. 77 (1973) 2049–2054.
[31] R.L. Gustafson, A.E. Martell, J. Phys. Chem. 67 (1963) 576–582.
[32] S.J. Lippard, H. Schugar, Ch. Walling, Inorg. Chem. 6 (1967) 1825–1830.
[33] H. Schugar, Ch. Walling, R.B. Jones, H.B. Gray, J. Am. Chem. Soc. 89 (1967) 3712–3720.
[34] H.J. Schugar, G.R. Rossman, C.G. Barraclough, H.B. Gray, J. Am. Chem. Soc. 94 (1972) 2683–2690.
[35] J.H. Carey, C.H. Langford, Can. J. Chem. 51 (1973) 3665–3670.
[36] L.H. Hall, J.L. Lambert, J. Am. Chem. Soc. 90 (1968) 2036–2039.
[37] P. Boule, M. Bolte, R. Richard, in: P. Boule (Ed.), Environmental Photochemistry, Springer, Berlin, Heidelberg, 1999, pp. 181–215.
[38] S. Metsärinne, P. Rantanen, R. Aksela, T. Tuhkanen, Chemosphere 55 (2004) 379–388.
[39] M.M. Darj, E.R. Malinowski, Anal. Chem. 68 (1996) 1593–1600.
[40] J.G. Calvert, J.M. Pitts Jr., Photochemistry, Wiley, New York, 1966, pp. 795–814.
[41] H. Schugar, A.T. Hubbard, F.C. Anson, H.B. Gray, J. Am. Chem. Soc. 90 (1969) 71–77.
[42] N. Tüfekci, H.Z. Sarikaya, Water Sci. Technol. 34 (1996) 389–396.
[43] F.J. Millero, Y. Wensheng, J. Aicher, Mar. Chem. 50 (1995) 21–39.
[44] W.L. Miller, D.W. King, J. Lin, D.R. Kester, Mar. Chem. 50 (1995) 63–77.
[45] J.M. Santana-Casiano, M. Gonzáles-Dávila, M.J. Rodríguez, F.J. Millero, Mar. Chem. 70 (2000) 211–222.
[46] K.D. Welch, T.Z. Davis, S.D. Aust, Arch. Biochem. Biophys. 397 (2002) 360–369.
[47] S. Seibig, R. van Eldik, Inorg. Chem. 36 (1997) 4115–4120.
[48] V. Zang, van Eldik, Inorg. Chem. 29 (1990) 1705–1711.